# RESULTS OF GEOPHYSICAL SCANNING OF A ROMAN SENATORIAL VILLA IN THE SANTA MARINA BAY (CROATIA, ISTRIA) USING THE AMPLITUDE DATA COMPARISON METHOD (ADCM)

**Fabian Welc[1*], Corinne Rousse[2], Gaetano Bencic[3]**

[1] *Institute of Archaeology, Cardinal Stefan Wyszynski University in Warsaw, Wóycickiego 1/3, bud. 23, 01-938 Warsaw, Poland; e-mail: f.welc@uksw.edu.pl*

[2] *Aix Marseille University, CNRS, Centre Camille Jullian, 5 rue du Château de l'Horloge BP 647, 13094, Aix-en-Provence, France; e-mail: corinne.rousse@univ-amu.fr*

[3] *Zavičajni Muzej Poreštine, Decumanus 9, 52440 Poreč, Croatia; e-mail: gaetano.bencic@muzejporec.hr*

*\* corresponding author*

**Abstract:**
The article presents application of the new geophysical amplitude data comparison method (ADCM), resulting from integrated geophysical survey using ground-penetrating radar (GPR) and magnetometry. The ADCM was applied to recognize the horizontal and vertical stratigraphy of a Roman senatorial villa located in Santa Marina (western part of Croatian Istria). The measurements were carried out in 2017−2019 at this site, accompanied by a use of GPR and gradientometer. These two methods significantly differ from each other, but on the other hand, they are complementary to some extent. This is due to the fact that the methods register different types of underground materials. The GPR records electromagnetic waves reflected from real buried remains or boundaries between geological or archaeological layers that differ significantly in electrical properties. The magnetic method, in turn, records the anomalies of the magnetic field intensity resulting from the underground concentration of ferromagnetic minerals, hence it is ideal for searching structures filled with organic matter or burning material. However, a separate usage of these methods does not guarantee a full picture of archaeological structures that are preserved underground. Only the application of the ADCM allowed for a comparison of GPR and magnetic amplitude data reading, following which a spatial image (2D and 3D) of the preserved archaeological structures and the geological stratigraphy of the Santa Maria site were obtained.

**Key words:** archaeology, geophysics, ground-penetrating radar, magnetometry, Roman period, Croatia

*Manuscript received 30 March 2020, accepted 21 April 2020*

## INTRODUCTION

The Santa Marina archaeological site in western Istria (Tar−Vabriga Municipality, Croatia) has been studied for several years by the Franco−Croatian archaeological mission (Aix Marseille University/Centre Camille Jullian, École Française de Rome, Poreč Zavičajni muzej Poreštine) (see Benčić *et al*., 2019; Kovačić *et al*., 2018; Rousse *et al*., 2019). In the course of the excavations, a part of a large senatorial and later Imperial maritime villa (1st−5th century AD) were discovered 400 m to the north of the well-known amphora workshop of Loron, which belonged to the same property (Tassaux *et al*., 2001). The villa occupied 5,000 m² and, although most structures are currently hidden by a forest, excavations in 2014−2019 and field reconnaissance since 2012 have revealed several buildings presenting the same orientations, erected on a slope facing the bay (see: on-line reports of the Ecole Française de Rome https://journals.openedition.org/). The seaward facade of the villa is emphasized by a long terrace wall, which delimits a sequence of rooms about a hundred meters long. The residential part of the villa expands above on the first terrace facing the sea. It is poorly known, with just two large rooms excavated in the northern sector of the villa. The upper terrace is occupied by a service quarter abutting a large cistern, and by olive oil mills and presses recently discovered to the south (in 2019 – not integrated in the plan below), which correspond to the rustical parts of the villa. Although the buildings are very levelled, the excavation has also provided a large number of varied objects (more than 3,000), which precisely indicate several phases of the villa development, from its construction in the beginning of the 1st century AD until its abandonment and demolition of the complex in the 4th−5th century (Rousse *et al*., 2016; Benčić *et al*., 2019).
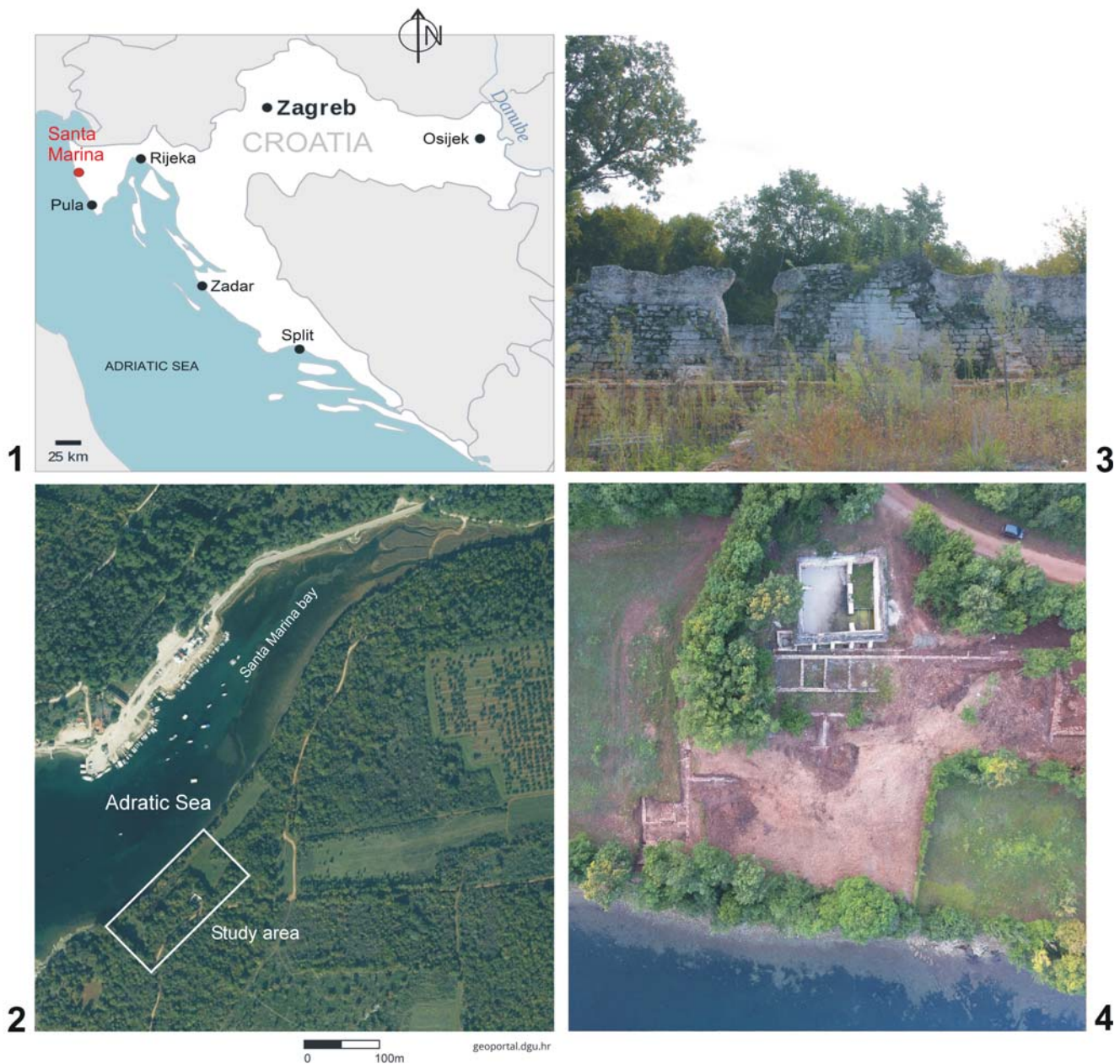
**Fig. 1.** 1: Location of the Santa Marina archaeological site (Drawing: F. Welc). 2: The area surveyed using magnetic and GPR methods covering the northern sectors of the Roman senatorial villa complex (After: Croatian Geoportal/Geoportal GDU: https://geoportal.dgu.hr/). 3: The Roman water cistern being the only still standing architectural feature belonging to the northern part of the Roman villa complex in Santa Marina (Photo: F. Welc). 4: The excavated fragment of the walls belonging to the northern compound of the villa (Photo: Corinne Rousse, Aix Marseille University, CNRS, Centre Camille Jullian in Aix-en-Provence).

During the last three years a geophysical survey was conducted at the site, headed by Fabian Welc in collaboration with the Poreč Zavičajni Muzej Poreštine and the Centre Camille Jullian of Aix Marseille University. The main goal was to determine the possible extension of the northern part of the villa using a ground-penetrating radar and magnetometry (Fig. 1). In course of the interpretation, a newly developed amplitude data comparison method (ADCM) resulting from an integrated geophysical survey was applied to recognize the horizontal and vertical stratigraphy of the remains.

## METHODS

### Introduction to the amplitude data comparison method (ADCM)

From a methodological point of view, the ADCM is based on comparing magnetic amplitude records from individual profiles with corresponding to them GPR reflection profiles. This allows to analyze the 3D aspects of buried features based on GPR images and their physical compo-
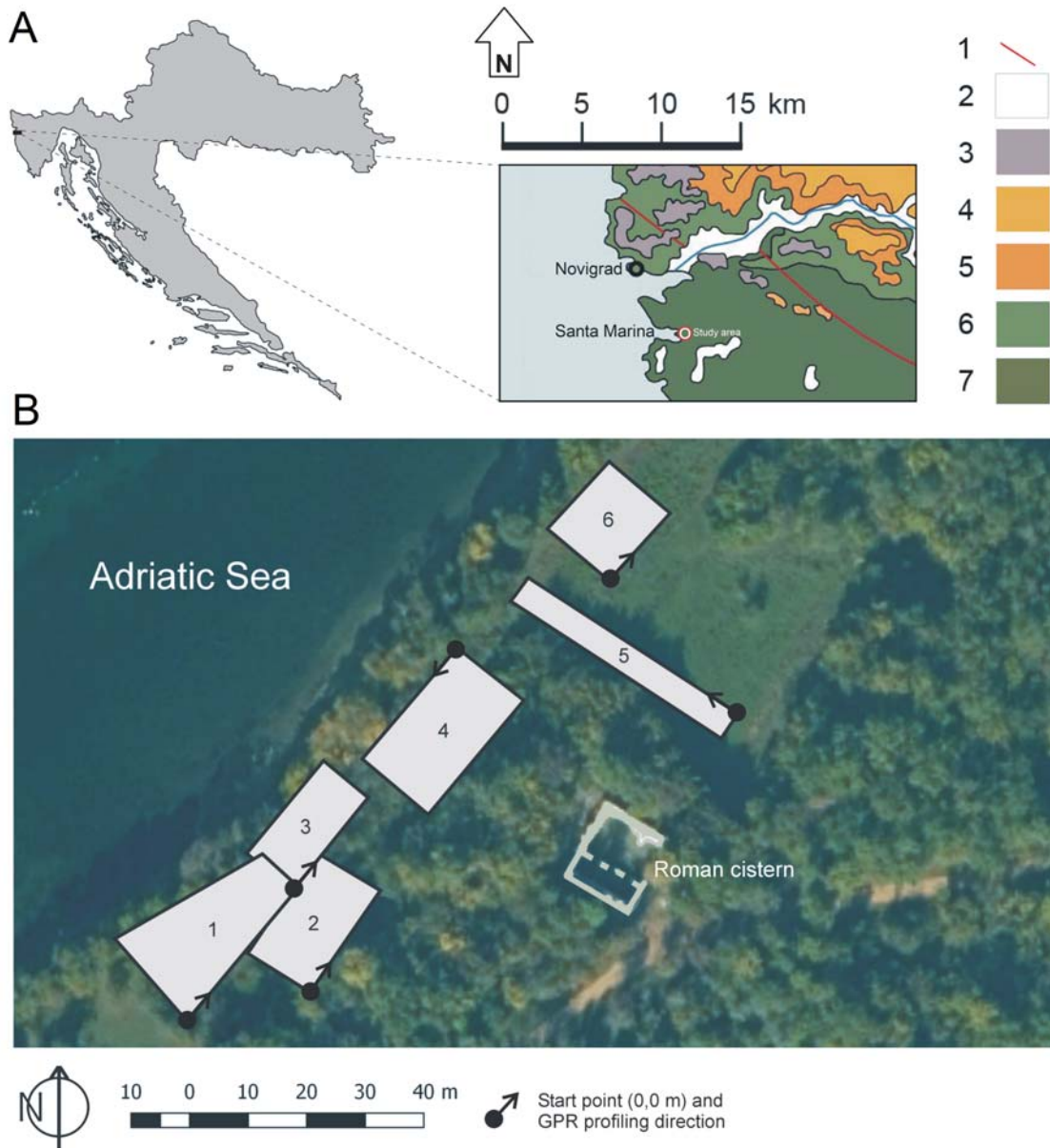
**Fig. 2.** A: Simplified geological map of Santa Marina area: 1 – faults, 2 – Quaternary deposits, 3 – Holocne Terra rossa deposits 4 – Eocene Flysch deposits, 5 – Paleocene and Eocene limestone deposits, 6 – Cretaceous limestone, 7 – Cretaceous limestone, dolomite and breccia deposits (After: Felja *et al.*, 2015, modified by F. Welc). B: Location of the GPR survey areas nos. 1 – 6 within the Santa Marina archaeological site (After: Croatian Geoportal/ Geoportal GDU: https://geoportal.dgu.hr).

sition from magnetic readings. As a result, the ADCM provides a more complete understanding of the buried archaeological objects and structures detected by geophysical surveys using the GPR method and magnetic gradiometry (Conyers, 2018; Welc *et al.*, 2019).

Magnetometry and GPR are the geophysical methods that are most often used in archaeological surveys. However, each of these methods has its own limitations and ambiguity, and the obtained results are strongly dependent on geology of a site, composition geometry of buried features and a variety of other physical and chemical characteristics (Welc *et al.*, 2019). The GPR method

is based on emitting electromagnetic waves (EM) with frequencies in the range of high and ultra-high frequency radio waves by a transmitting antenna and a steering device. At a boundary between two geological or archaeological layers, significantly differing in electrical properties (mainly electric permeability = dielectric constant – $\varepsilon_r$), the electromagnetic wave is reflected and then recorded by the radar's receiving antenna. The reflection coefficient (R) of the EM wave is equal to the ratio of the reflected wave amplitude to the amplitude of the wave falling on the boundary of two layers differing in the dielectric constant (Karczewski, 2007):

$$R = \frac{\sqrt{\varepsilon_{r_2} - \varepsilon_{r_1}}}{\sqrt{\varepsilon_{r_2} + \varepsilon_{r_1}}}$$

Unlike the GPR method, magnetometry uses measurements of a geomagnetic field intensity. About 90% of the Earth's total magnetic field is generated within it and referred to as the main field (Anovskij, 1978). The observed magnetic field value measured at a specific place and time ($F_{obs}$) is the sum of magnetic fields of different origin (dipolar field – $F_D$, continental field – $F_C$, external-extraterrestrial field – $F_E$, anomalous field – $F_A$ and rapidly changing fields – $\delta F$). The dipole and the continental fields, which account for 80% and 10−20% of the Earth's magnetism, respectively, have the largest share. The sum of these fields determines the value of the Earth's main magnetic field (Grabowska, 2012):

$$F_M = F_D + F_C$$

The geomagnetic field describes the total intensity vector ($\overrightarrow{F}$) which consists of horizontal ($\overrightarrow{H}$) and vertical ($\overrightarrow{Z}$) components expressed in nanoteslas (nT), inclination (I) and declination (D) (Grabowska, 2012). The magnetic anomaly ($\Delta F$) is the difference between the measured value ($F'_{obs}$), which is the observed total magnetic field without a rapidly changing field (e.g. diurnal changes) and the value of the normal field Fn, taken from the International Geomagnetic Reference Field model or calculated as an average value of the magnetic field in a given area (Grabowska, 2012):

$$\Delta F = F'_{obs} - Fn$$

where: $F'_{obs} = F_{obs} - \delta F$ (rapidly changing field value) (Grabowska, 2012).

In the field, the total intensity values and components of the geomagnetic field are measured using different types of magnetometers (e.g. proton precession, optically pumped, cryogenic) or magnetic gradientometers. Gradientometers (gradiometers) are measuring devices very often used in archaeological prospection. In this case horizontal or vertical derivatives of the total magnetic intensity are obtained by measurements and comparison of two values of the geomagnetic field (or its components) in two closely situated points, up to 1.5 m. The results of measurements taken by means of gradiometers are expressed in nanoteslas per meter (nT/m). The principles of gradiometer operation allow for the elimination of the normal magnetic field from the measurements and are highly resistant to any interference of the magnetic field (Fassbinder, 2015, 2017).

Anomaly maps produced by gradiometers and magnetometers present mostly concentrations of ferromagnetic minerals such as metal objects, fireplaces or burned materials (Fassbinder and Stanjek, 1993; Gaffney, 2008; Fassbinder, 2015, 2017; Welc *et al.*, 2019). Anomalies strictly connected with archaeological features are usually very weak and can be measured in values of a few nT – in comparison to the magnetic field intensity (Grabowska, 2012) presently at ca. 48 000 nT in the study area in Croatia. Features (intensity, shape, direction of magnetic anomalies, gradient zones) observed on magnetic anomaly maps exhibit two main types of magnetization: remanent (materials or sediments which retain past magnetism) and induced (buried material or sediment enriched with fine-grained magnetic particles affected by the currently existing geomagnetic field). When sediments or other objects are exposed to high temperatures, they become magnetized by thermoremanent magnetization (TRM) (Fassbinder, 2015, 2017).

While the magnetic minerals are cooled through their critical temperatures (e.g. Curie temperature of magnetite ca. 580ºC), their magnetization is usually aligned with the current direction of the Earth's magnetic field (Fassbinder, 2015). Because all types of the soils are characterized by their more or less magnetic properties (magnetization, magnetic susceptibility) and enhanced magnetization of a magnetically enriched topsoil is a typical phenomenon (Armstrong *et al.*, 2012; Fassbinder, 2015; Łyskowski *et al.*, 2018; Wojas, 2017), hence archaeological structures refilled by topsoil generate a distinctive positive magnetic anomaly on magnetograms. In contrast, negative anomalies may have numerous reasons (Fassbinder, 2017; Welc *et al.*, 2019). The most common situation is when the material of the archaeological structure possesses a lower magnetic susceptibility than for example, the adjacent topsoil (Welc *et al.*, 2017).

The magnetic method alone is not suitable for understanding the vertical archaeological stratigraphic sequence of buried features and structures that might be of different ages (Fassbinder, 2015, 2017). It provides only a plan of the archaeological site in the form of the deviation (amplitude) of the absolute value of the magnetic field, so there is no third dimension – depth (Herwanger *et al.*, 2000). Only when individual GPR reflection profiles are interpreted together with associated magnetic values, it is possible to interpret types of materials visible in the GPR profiles and these two datasets become complementary (Conyers, 2018; Welc *et al.*, 2019). At Santa Marina, the ADCM turned out to be the most efficient to understand what induces specific kinds of anomalies. For the ADCM purpose, selected GPR reflection profiles recorded at Santa Maria were combined with corresponding gradiometer readings extracted from parallel magnetic profiles. The next step was the analysis of visible anomalies and determination of their character based on GPR images and their magnetic signatures (Conyers, 2018; Welc *et al.*, 2019).

**GPR survey methodology and data processing**

During geophysical surveys performed at Santa Marina, the GPR system ABEM/Malå Groundexplorer was used. The prospection was carried out with application of a screened transmitting bimodal antenna, with nominal frequency of the emitted EM wave at 450 MHz. All obtained reflection
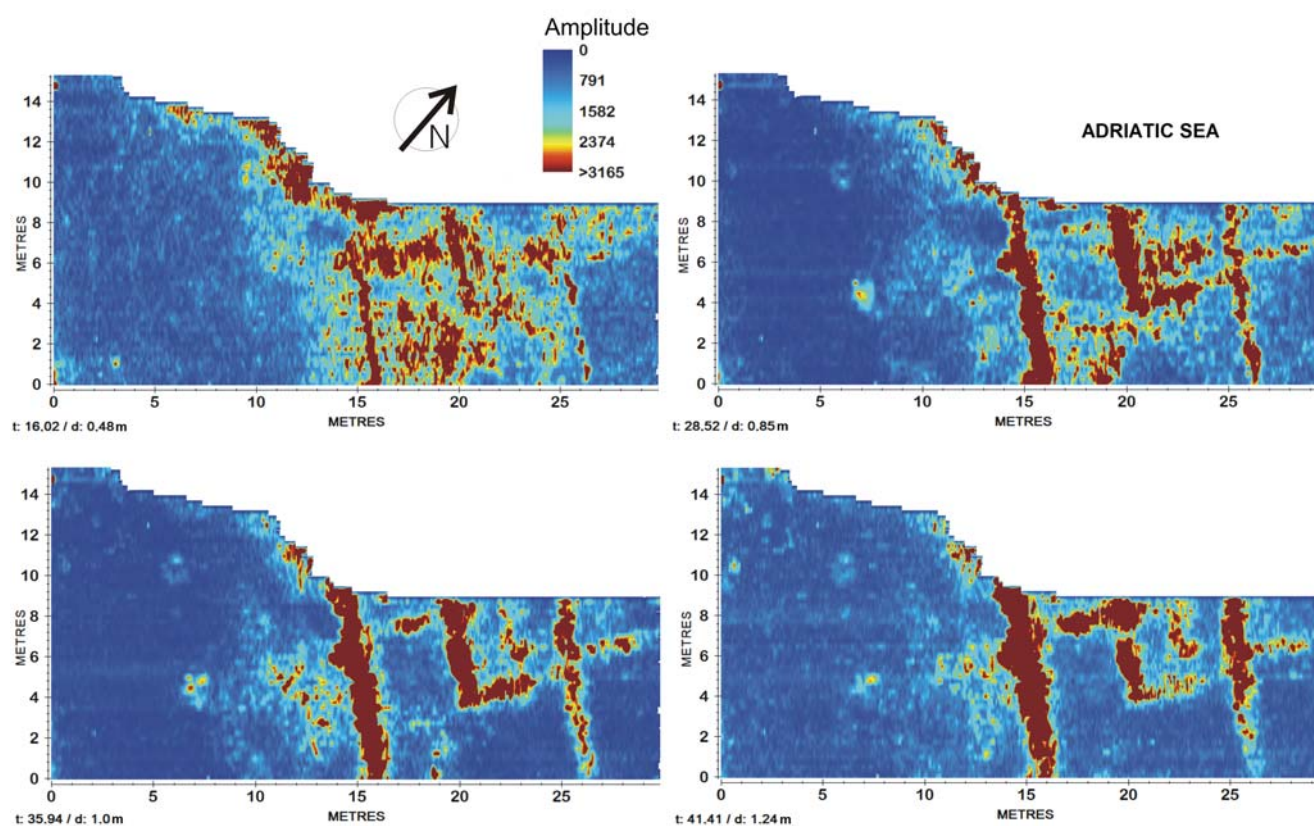
**Fig. 3.** GPR survey results for survey area no. 1 (studied in 2017). Time-slices (= GPR maps) prepared for depth range 0.48–1.24 m (Processing and drawing: F. Welc).

profiles were later processed with Reflex-Win (www.sand-meier-geo.de). A number of processing procedures were applied; their main aim was the enhancement of the usable signal in relation to the background, i.e. noise: *Running average*, *Dewow* (variant of the *running average* procedure), *Subtract-mean*, *Gain*, *Move start time*, *Bandpass frequency*, *Background removal* and *Average xy filter*. The last procedure of data processing arranged the reflection profiles in quasi 3D block-diagrams using the Reflex View *3D data interpretation* mode. Several indispensable procedures were used to prepare the 3D block-diagrams.

**Magnetic gradiometry survey methodology and data processing**

A high-resolution fluxgate gradiometer Grad601 produced by Bartington Instruments Co. was used during the survey at Santa Marina. All profiles were separated from each other at 0.5 m. The effects of magnetic measurements are presented here in the form of black and white distribution maps of magnetic anomalies. The positive scale means that the darker areas correspond to anomalies with higher magnetic field values, while the light areas point to lower values. In other words, the blackened areas indicate greater concentrations of matter or sediment enriched in ferromagnetic minerals. In most cases these areas are an effect of extensive past human activity.

**GEOLOGICAL AND GEOMORPHOLOGICAL BACKGROUND**

From a structural point of view, the archaeological site at Santa Marina is located in the western part of Istria and belongs to the External Dinarides, composed mostly of limestones deposited on the Adriatic Carbonate Platform and dated from the Early Jurassic to the Eocene (Velić *et al*., 2002). The Istrian carbonate series consists mostly of rocks dating from the Middle Jurassic to the late Eocene, with subordinate middle to upper Eocene clastic rocks comprising flysch and calcareous breccias (Tišljar *et al*., 1998; Felja *et al*., 2015; Vlahović *et al*., 2005) (Fig. 2A).

In order to derive the proper conclusions from the usage of the ADCM, it is necessary to determine magnetic characteristics of a soil and magnetic prosperities of the archaeological constructions preserved at the Santa Marina site. The whole area is dominated by a characteristic reddish clayey-sandy deposit with a well-developed terra rossa soil at the top. Such soil developed mostly on Jurassic–Cretaceous–Paleogene carbonate rocks. In most cases, the soil has a polygenetic origin and was formed by mixing of insoluble residues of carbonate rocks with weathered and eroded loess and flysch sediments (Durn, 1996; Durn *et al*., 1999). The characteristic red colour of the terra rossa in Istria, as well as in other regions, results from a high content of haematite and goethite. These two minerals constitute the main pedogenic iron oxide phases
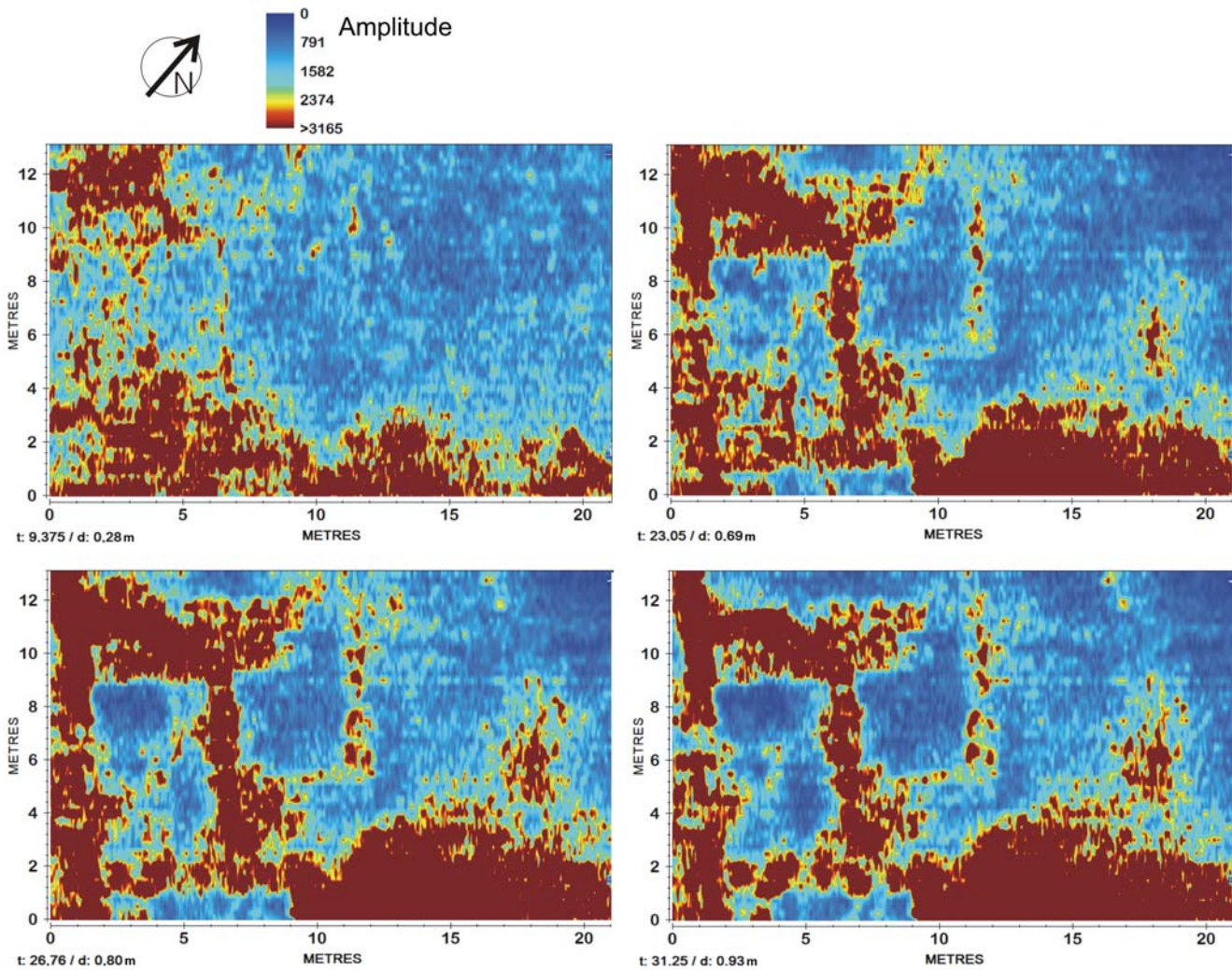
Fig. 4. GPR survey results for survey area no. 2 (2018/1). Time-slices prepared for depth range 0.28–0.93 m (Processing and drawing: F. Welc).

in terra rossa soils (Durn, 2003). In 2018, during a field survey of the Santa Marina site, magnetic susceptibility (MS) measurements were performed directly on surfaces of stone structures exposed in archaeological trenches and using bulk of the sediments. The stone walls are mainly made of limestone, whose magnetic susceptibility values range from 0.01 to 0.09 × SI units. Rich in iron oxides, the sandy-clayey terra rossa sediments surrounding the stone structures are characterized by much higher magnetic susceptibility values – from 1.07 to 1.74 × SI units. As a result, the Roman stone walls are visible on magnetic maps as areas with reduced magnetic field intensity relative to the background. Unfortunately, a large content of clay in terra rossa makes significant suppression of the EM waves and thus reduces the GPR depth range.

## RESULTS OF APPLICATION OF ADCM

The most important data were delivered at Santa Marina by survey areas 1–3, located 60 m to the SW of the Roman
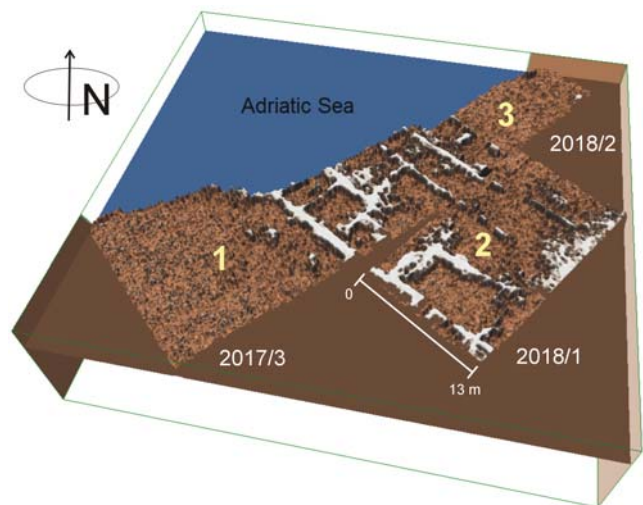


Fig. 5. 3D model of the ancient Roman structures discovered within survey areas nos. 1–3 based on GPR survey results (depth ca. 0.7 m) (Drawing: F. Welc).
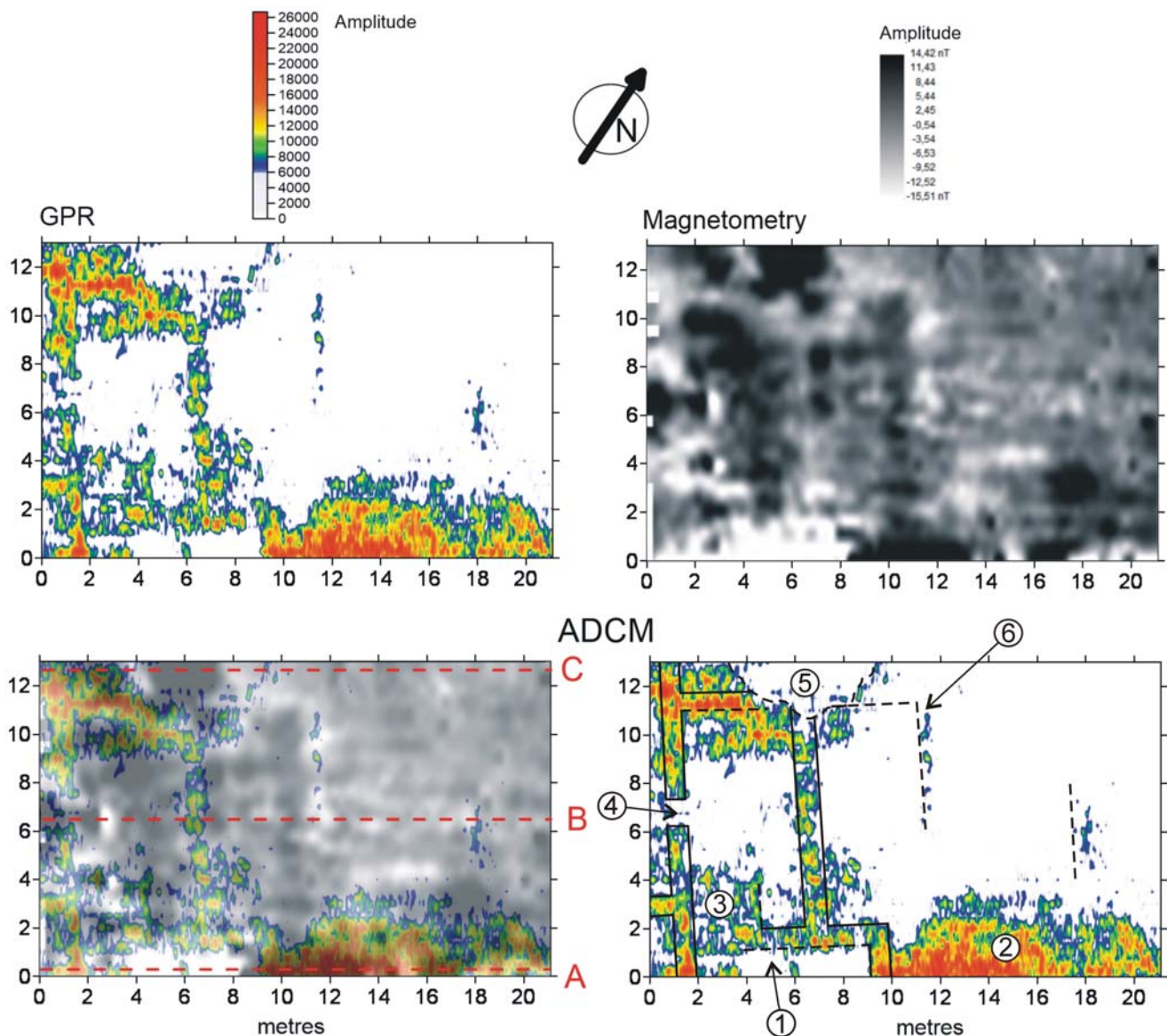
Fig. 6. ADCM analysis of survey area no. 2. Upper left: GPR slice prepared for the depth of 0.7 m. Upper right: results of magnetic survey. Lower left: superimposed GPR and gradiometer survey results. Lower right: ADCM interpretation: 1 – rectangular room filled with fine limestone rubble, 2 – depression filled with stone rubble mixed with organics and ashes, 3 – probable kiln construction, 4 – entrance to the compound, 5 – depression filled with a highly magnetic content (ashes and organics), 6 – partially preserved limestone walls (Processing, interpretation and drawing: F. Welc).

cistern along a sea shoreline (Fig. 2B). GPR measurements were performed with additional gradientometer profiling made within the survey area 2. (Figs 3–4). The obtained GPR time-slices (GPR amplitude value maps) have revealed characteristic high amplitude linear anomalies oriented along the NW-SE axis and recorded at 0.5–1.5 m depth (Fig. 5). They are generated by shallowly buried stone walls belonging to the northern part of the Roman senatorial villa compound. Results of the additional magnetic survey performed within the survey area 2 present numerous features marked by high values of magnetic field intensity (above 6 nT) and most probably, they are generated by concentration of organics and ashes. For ADCM analysis, GPR reflection profiles marked as A, B and C taken from the survey area

were selected and combined with the corresponding gradiometer readings (Fig. 6). It is very important to note that the maximum depth of magnetic anomalies can be estimated at ca. 1 m, which corresponds to the maximum range depth of gradiometer prospection.

Analysis of the GPR reflection profile labeled as A (Fig. 6) and the corresponding magnetic amplitude values has revealed numerous features, which can be connected with a vertical stratigraphy of the Roman villa. Between the $3^{rd}$ and $10^{th}$ m of the GPR profile at 0.5–1.0 m depth, there is a zone of electromagnetic wave attenuation (Fig. 7A: 1), reflected on the magnetic parallel profile by low values of magnetic readings (from 0 to -10 nT). This anomaly can be interpreted as an infilling of a room in the Roman building,
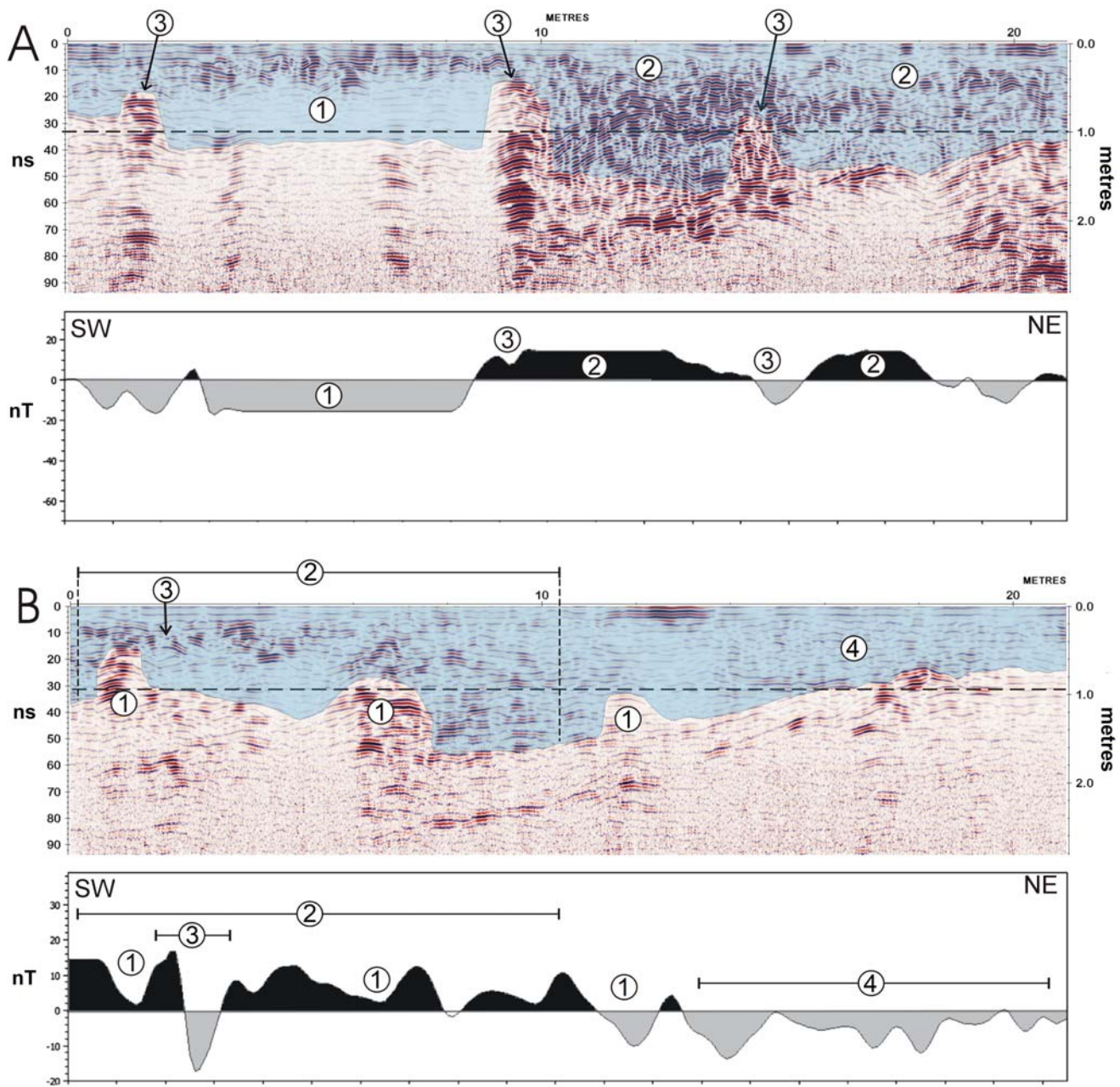
Fig. 7. Results of ADCM analysis of selected GPR profiles and corresponding magnetic records for survey area no. 2. Profile A: 1 – non-magnetic sediments filling a room in the Roman building. 2 – vast depression filled with more magnetic and coarser material (sands and stone rubble) mixed with organics and ashes. 3 – location of the upper part of the limestone walls. Profile B: 1 – cross-section through limestone walls. 2 – shallow depressions filled with diverse and highly magnetic material. 3 – dipole anomaly, burning place? 4 – shallow hollow filled with slope sediments, mainly sands and fine limestone debris (Processing, interpretation and drawings: F. Welc).

composed of a mixture of sand and clay. It suggests that the interior of the building was left unearthed for some time to about 1 m below the ground. As a result, it became gradually (in the long term) and naturally filled with the flowing sediments.

At the depth of about 1 m – between $10^{th}$ and $20^{th}$ m of the same profile, there are numerous horizontal and oblique reflective surfaces, which correspond to particular phases of infilling of a vast depression located further to the north of the Roman structure (Fig. 7A: 2). This feature is marked

on the corresponding magnetic profile as a high amplitude magnetic zone (from 0 up to 18 nT). Therefore, sediments that fill this depression contain most probably much magnetic matter, mostly organics and ashes. Additionally, the mentioned numerous horizontal and oblique GPR reflection indicates that the hole is filled with packages of coarse material, most probably sands and fine stone debris. Between ca. 0.5 and 1 m below the surface, on the $3^{rd}$, $8^{th}$ and $14^{th}$ m of the GPR profile, there are concentrations of diffraction hyperbolas (Fig. 7A: 3), indicating location of
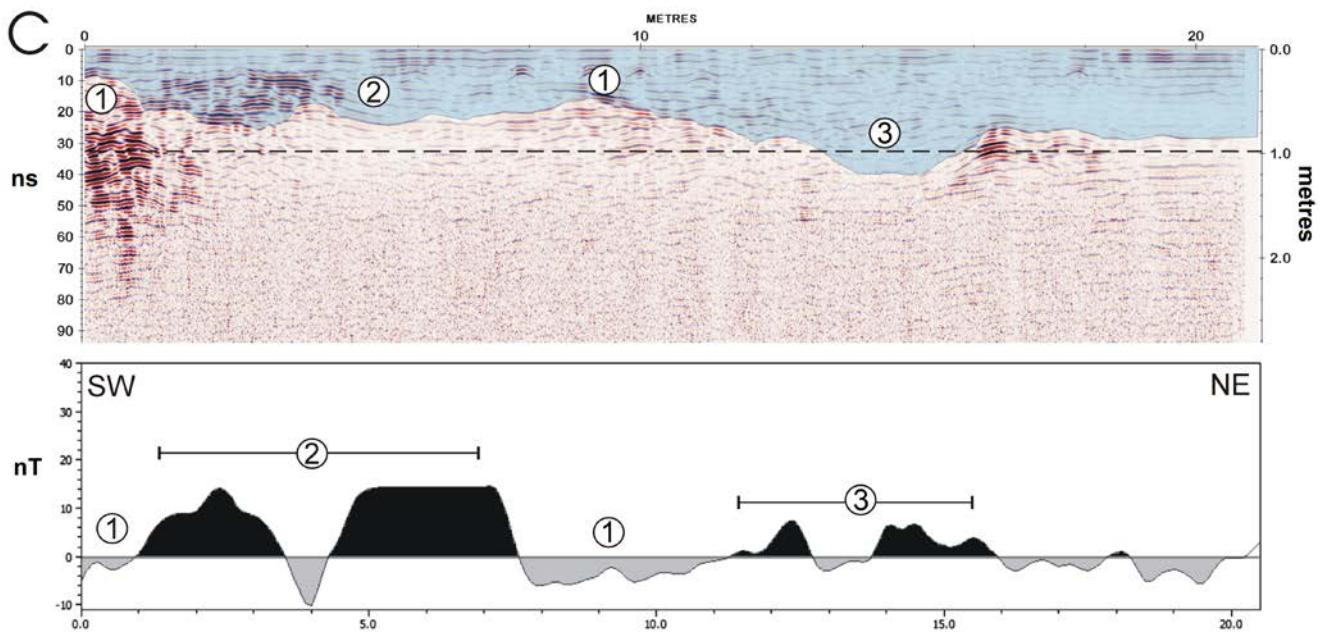
Fig. 8. Results of ADCM analysis of the GPR profile labelled as C from survey area no. 2: 1 – location of remains of the limestone walls, which correspond to lower magnetic amplitude values. 2 – shallow depression between the walls, filled with organic matter and possibly burnt material, 3 – an analogous depression located further to the NE (Processing, interpretation and drawing: F. Welc).

the upper part of the stone walls. These features correspond to lower magnetic amplitude values, because all walls were made from a non-magnetic limestone.

The GPR reflection profile labelled as B revealed a cross-section through three limestone walls, manifested as a set of reflection hyperbolas at 0.5–1 m depth (Fig. 7B: 1). In magnetic records, these places are characterized by a slight decrease in amplitude values. The space between these walls is occupied by shallow (up to 1.5 m) depressions filled with diverse and magnetic material, which is attested by high magnetic readings (most probably silty sands, re-deposited terra rossa, organics and ashes) (Fig. 7B: 2). A distinctive reflection surface at approximately 0.5 m depth (Fig. 7B: 3) occurs in the SW part of the GPR profile. A characteristic dipole anomaly is visible in this place on the magnetic profile, which may suggest a burning place. A wide zone characterized by a low value of the amplitude signal occurs between the 12th and 22nd m of the GPR profile, which harmonizes with lower values of the magnetic amplitude. Therefore, this zone can be interpreted as a vast and shallow hollow filled with non-magnetic sediments, mainly sands, and fine and very fine limestone debris (Fig. 7B: 4).

The last analyzed GPR profile, labeled as C (Fig. 8), reveals a stratigraphy similar to profiles A and B. The GPR signal boost zones are slightly less pronounced in places of stone walls (Fig. 8: 1), which corresponds to lower magnetic amplitudes. A shallow depression is visible between the walls, most probably filled with organic matter and possibly burnt material, which can be judged by a corresponding high value of the magnetic amplitude (Fig. 8: 2). An analogous depression is filled with organics and ashes, visible between the 12th and 15th m of both profiles (Fig. 8: 3).

The area, located immediately north of survey areas and labelled as the survey area 4, was tested using the GPR method. All profiles were measured at distances of 0.4 m using an antenna with a nominal frequency of 450 MHz (Fig. 9). Time-slices prepared for the depth interval of 0.3–1.0 m, present in the SE and S part of the survey area linear anomalies, produced by the top of a solid stone wall. The feature belongs undoubtedly to the Roman villa complex. Time-slices prepared based on GPR surveys within areas 5 and 6 have also outlined a series of stone walls at different orientations, which form another, SE part of the Roman villa structure (Fig. 9).

## DISCUSSION

Within the low terrace along the sea coast in Santa Marina, six survey areas for geophysical measurements (using GPR and magnetic methods) were selected. The GPR system ABEM/Malå Groundexplorer was used during the survey (Fig. 2). The prospection was carried out with application of a screened transmitting bimodal antenna, with a nominal frequency of the emitted EM wave at 450 MHz. The survey was supplemented by gradiometer measurements performed in survey area 2. In the following step, collected magnetic and GPR data were used to analyze the stratigraphy of the site using the ADCM. The produced GPR time-slices, reflection profiles and magnetic maps clearly indicate that the integration of these two methods allows for a detailed and effective identification of buried archaeological structures in a 3D perspective. GPR time-slices prepared for the depth range from 0.5 m downwards
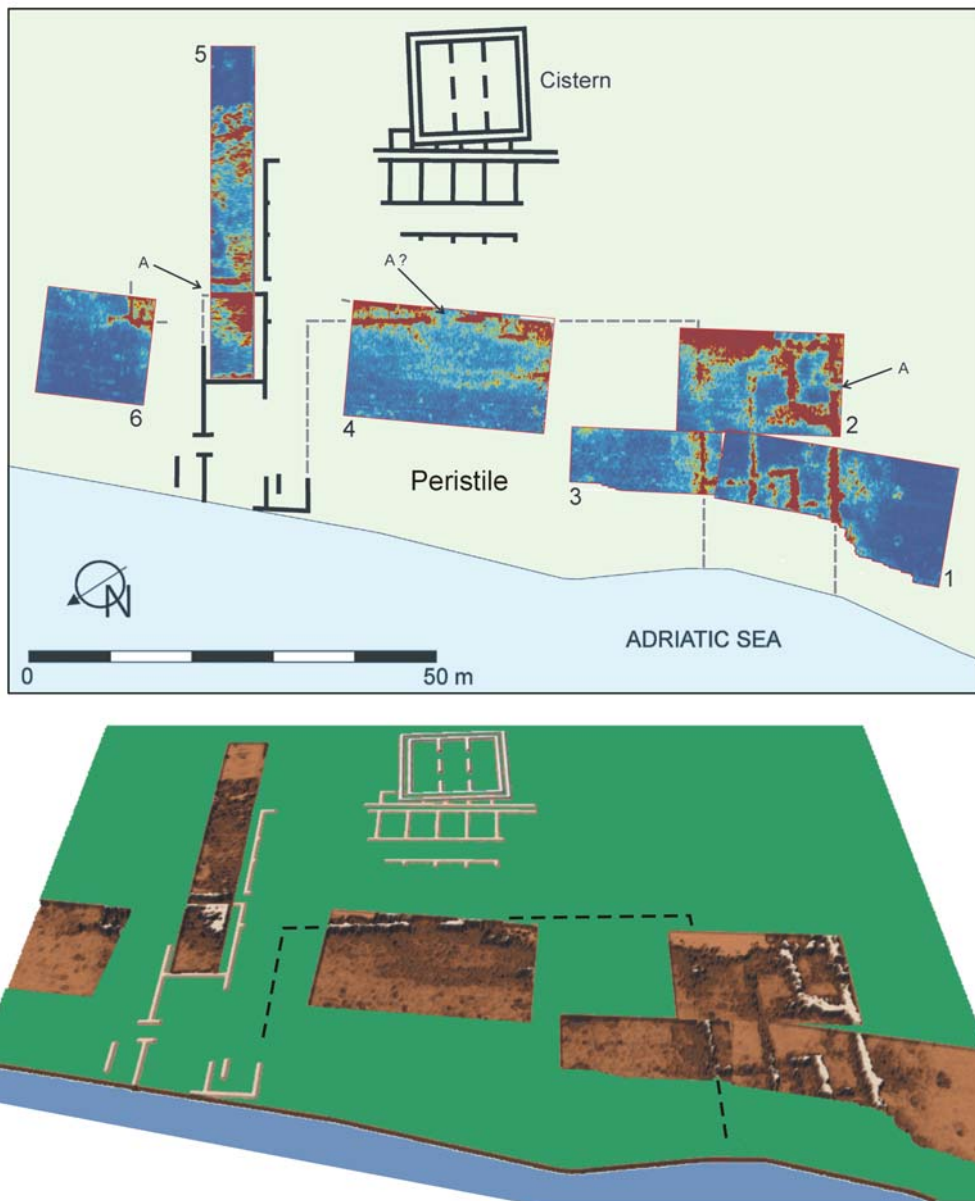
Fig. 9. Results of the GPR survey in Santa Marina. Upper: location of survey areas nos. 1–6 and architectural features discovered during excavations. A possible entrances to the villa compound. Lower image: 3D model of discovered structures with outline of vast courtyard of the villa (Interpretation and drawings: F. Welc).

reveal numerous distinctive NW–SE and SW–NE-oriented linear anomalies, which are generated mostly by shallow buried limestone walls. The wall remains belong undoubtedly to the senatorial Roman villa complex. The outline of the stone remains preserved on the sea shore indicates that they continued seawards, which confirms much lower sea levels in Roman times compared to the present-day level.

The plan and distribution of the structures excavated around the Roman cistern combined with selected GPR slices revealed the outline of a vast courtyard or more probably – a peristyle surrounded by two wings with several rooms of different sizes. There is one main entrance leading from the NE (Fig. 9), probably presenting a set of external buttresses or reinforcements, which would suggest that the complex of the villa might not have spread further

to the SW. Certainly, worth noting is possible reworking of certain spaces, detected by shallower time-slices and by the ADC method. Likewise, features such as hearths and burning residues might suggest a subsequent use of parts of the structures. These details should, however, be confirmed by new excavations (Fig. 9).

The performed ADCM analysis of data delivered from survey areas 2 and 4 allowed for initial recognition of horizontal and vertical stratification of the site. The analyzed GPR profiles with corresponding magnetic values enabled distinguishing two main stratigraphic horizons, the upper from 0 to approximately 1 m, and the lower <1 m. The first one can be connected with a period of demolition of the villa precinct in the time span from late antiquity to the present. Anomalies produced by holes and

depressions filled with ashes, organics, reworked top-soil and stone rubble dominate on this depth. There are also characteristic planar anomalies reflecting boundaries between packages of sediments brought down along a local slope. In result, shallow subsurface layers in the study area seem strongly disturbed. Archaeological trenches dug in the vicinity of the area have revealed soil zones with a low content of humus (organic material) and at least one generation of slope series, which consist mainly of brown silty and vari-grained sand. Massive structure and lack of gradation is characteristic for this sediment. Organic matter is dispersed in all genetic horizons. It is related to the extraction of silty and clay fractions and organic matter during intensive water runoff caused by periodically volatile rainfall. With high probability it can be assumed that partly natural and partly artificial narrow terraces along the coast were created in post-antiquity times as a result of large-scale mass movements (see, Welc, 2019). In effect, all ancient structures located near the seashore were covered by slope sediments, which now cover the Roman remains in the bay. It is very interesting to note that the time of deposition of the slope deposits covering the remains of the Roman building is reflected in the drilling S-2 performed in the Santa Marina Bay (Faivre *et al.*, 2011). Marine series in a core are overlain by characteristic red clays followed by a red soil at 0.04 m depth. Presence of this sediment was explained as result of colluvial (slope) processes. An intensive red colour indicates their formation by erosion of terra rossa from the carbonate surroundings of the Santa Marina Bay. Analysis of other Holocene drill cores from the western coast of the central Adriatic proved that similar slope sediments are a result of deforestation that took place around 700 BP (early Middle Ages) (Oldfield *et al.*, 2003). Each episode led to deposition of mass wasting sediments as a response of surface processes to widespread forest clearance and maybe also climate changes. The most intensive slope processes are dated between 1100 and 700 yrs. BP (Oldfield *et al.*, 2003). A similar time interval should be considered for deposition of the red slope sediments that covered the Roman remains at Santa Marina. Below 1 m all GPR plans and reflection profiles present much clearer geophysical images of the underground features. Anomalies that should be interpreted as solid NW−SE-oriented stone walls are present on the GPR profiles. This set of walls defines the outline of a rectangular courtyard with an entrance from the SW.

## CONCLUSIONS

Measurements carried out in 2017–2019 in two survey areas at Santa Marina Bay provided the layout for the southern part of the Imperial phase of the previously established villa, possibly marking also its southern boundary by detecting presence of the entrance. Moreover, it probably established existence of the later (late Antique) phase of usage of the spaces, perhaps marked by some readaptations and changes in use.

## REFERENCES

Anovskij, B.M., 1978. Zemnoj magnetyzm. Izdatelstvo Leningradskogo Universiteta, Leningrad, 23–258.

Armstrong, A., Quinton, J., Maher, B., 2012. Thermal enhancement of natural magnetism as a tool for tracing eroded soil. Earth Surface Processes and Landforms 37, 14–20.

Benčić, G., Maggi, P., Rousse, C., 2019. La cisterna della villa di Santa Marina presso il complesso produttivo di Loron (Torre Abrega – Tar Vabriga, Croazia), dans G. Cuscito (dir.), Cura aquarum. Adduzione e distribuzione dell'acqua nell'antichità, Antichità, Altoadriatiche 88, 397–418.

Conyers, B.L., 2018. Ground-penetrating Radar and Magnetometry for Buried Landscape Analysis. Springer Briefs in Geography. Springer International Publishing, 121 pp.

Durn, G., 1996. Podrijetlo, sastav i uvjeti nastanka terra rosse Istre. Doctor Disertation, Zagreb, 204 pp.

Durn, G., 2003. Terra Rossa in the Mediterranean Region: Parent Materials, Composition and Origin. Geologia Croatica 56 (1), 83–100.

Durn, G., Ottner, F. Slovenec, D., 1999. Mineralogical and geochemical indicators of the polygenetic nature of terra rossa in Istria, Croatia. Geoderma 91, 125–150.

Faivre, S., Fouache, E., Ghilardi., M., Antonioli., F., Furlani, S., Kovačić, V., 2011. Relative sea level change in Istria (Croatia) during the last 5 ka. Quaternary International 232, 132–143.

Fassbinder, J.W.E., 2015. Seeing beneath the farmland, steppe and desert soil: magnetic prospecting and soil magnetism. Journal of Archaeological Science 56, 85–95.

Fassbinder, J.W.E., 2017. Magnetometry for archaeology. In: Gilbert, S., Allan, S. (Eds), Encyclopedia of Geoarchaeology. Springer, 499–515.

Fassbinder, J.W.E., Stanjek, H., 1993. Occurrence of bacterial magnetite in soils from archaeological sites. Archaeologia Polona 31, 117–128.

Felja, I., Fontana, A., Furlani, S., Bajraktarević, Z., Paradžik, A., Topalović, E., Rossato, S., Ćosiović, V., Juračić, M., 2015. Environmental changes in the lower Mirna River valley (Istria, Croatia) during the Middle and Late Holocene. Geologia Croatica 68/3, 209–224.

Gaffney, C.F., 2008. Detecting trends in the prediction of the buried past: a review of geophysical techniques in archaeology. Archaeometry 50, 313–336.

Grabowska, T., 2012. Magnetometria stosowana w badaniach środowiska. Wydawnictwa AGH, Kraków, 266 pp.

Herwanger, J.H., Maurer, A.G., Green, J., Leckebusch., 2000. 3-D inversions of magnetic gradiometer data in archaeological prospecting: possibilities and limitations. Geophysics 65 (3), 849–860.

Karczewski, J., 2007. Zarys metody georadarowej. AGH, Kraków, 346 pp.

Kovačić, V., Rousse, C., De Leonardis, V., Gergeta, G., Maggi, P., Taffetani, C., 2018. New research around the ceramic workshop of Loron (Tar-Vabriga, Croazia): the villa maritima located, dans Roman ceramics and glass manufactures: production and trade in

the Adriatic region. III International Archaeological Colloquium (Crikvenica 2014), Crikvenica, 68–73.

Łyskowski M., Pasierb B., Wardas-Lasoń M., Wojas A., 2018. Historical anthropogenic layers identification by geophysical and geochemical methods in the Old Town area of Krakow (Poland). Catena 163, 196–203.

Oldfield, F., Asioli, A., Accorsi, C.A., Mercuri, A.M., Juggins, S., Langone, L., Rolph, T., Trincardi, F., Wolff, G., Gibbs, Z., Vigliotti, L., Frignani, M., van der Post, K., Branch, N., 2003. A high resolution late Holocene palaeoenvironmental record from the central Adriatic Sea. Quaternary Science Reviews 22, 319–342.

Rousse, C., Munda, D, Benčič, G., Gergeta Sotončić, K., De Leonardis, V., Dumas, V., Maggi, P., Tillier, M., Vaschalde, Ch., 2016. Loron/Santa Marina-Busuja (Tar-Vabriga, Poreč, Croatie). Chronique des activités archéologiques de l'École française de Rome Balkans 2016, 1–16.

Rousse, C., Munda, D, Benčič, G., Maggi, P., Dumas, V., 2019. Loron/Santa Marina-Busuja (Tar-Vabriga, Poreč, Croatie). Chronique des activités archéologiques de l'École française de Rome Balkans 2019, 1–34.

Tassaux, F., Matijašić, R., Kovačić, V., 2001. Loron (Croatie). Un grand centre de production d'amphores à huile istriennes (Ier-IVe s. P.C.). Mémoires 6. Institut Ausonius, Bordeaux, 363 pp.

Tišljar, J., Vlahović, I., Velić, I., Matićec, D., Robson, J., 1998. Carbonate facies evolution from the late Albian to middle Cenomanian in southern Istria (Croatia): influence of synsedimentary tectonics and extensive organic carbonate production. Facies 38, 137–152.

Velić, I., Vlahović, I., Matićec, D., 2002. Depositional sequences and Palaeography of the Adriatic Carbonate Platform. Memorie Della Societa Geologica Italiana 57, 141–151.

Vlahović, I., Tišljar, J., Velić, I., Matićec, D. 2005. Evolution of the Adriatic Carbonate Platform: Palaeogeography, main events and depositional dynamics. Palaeogeography, Palaeoclimatology, Palaeoecology 220, 333–360.

Welc, F., 2019. Geoarchaeological evidence of the late and post-antiquity (5th–9th c. AD) climate changes recorded at the Roman sites in Plemići Bay (Zadar Region, Croatia). Studia Quaternaria 36 (1), 3–17.

Welc, F., Mieszkowski, R., Lipovac Vrkljan, G., Konestra, A., 2017. An attempt to integration of different geophysical method (magnetic, GPR and ERT): a case study from the late Roman settlement on the Island of Rab in Croatia. Studia Quaternaria 34 (1), 47–59.

Welc, F., Nebelsick, L.D., Wach., D., 2019. The first Neolithic roundel discovered in Poland reinterpreted with the application of the geophysical Amplitude Data Comparison (ADC) method. Archaeological Prospection 26 (4), 283–297.

Wojas, A., 2017. The magnetic susceptibility of soils in Krakow, southern Poland. Acta Geophysica, 65 (3), 453–463.